Theor Chem Acc (2004) 111:154–161
DOI 10.1007/s00214-003-0519-2

Theoretical
Chemistry Accounts

Regular article

Theoretical study of the S_N2 reaction of $Cl^-(H_2O) + CH_3Cl$ using our own *N*-layered integrated molecular orbital and molecular mechanics polarizable continuum model method (ONIOM – PCM)

Sung J. Mo[1], Thom Vreven[1,2], Benedetta Mennucci[3], Keiji Morokuma[1], Jacopo Tomasi[3]

[1] Cherry L. Emerson Center for Scientific Computation and Department of Chemistry, Emory University, Atlanta, GA 30322, USA
[2] Gaussian, Inc., 340 Quinnipiac Street, Building 40, Wallingford, CT 06492, USA, e-mail: thom@gaussian.com
[3] Dipartimento di Chimica e Chimica Industriale, Universita di Pisa, via Risorgimento 35, 56126 Pisa, Italy

Received: 24 March 2003 / Accepted: 5 May 2003 / Published online: 23 February 2004

Abstract. The effects of solvation in the S_N2 reaction $Cl^-(H_2O) + CH_3Cl$ were investigated using our own *N*-layered integrated molecular orbital and molecular mechanics (ONIOM) polarizable continuum model (PCM) method [Vreven T, Mennucci B, da Silva CO, Morokuma K, Tomasi J (2001) *J Chem Phys* 115:62–72], which surrounds the microsolvated ONIOM system with a polarizable continuum. The microsolvating water molecule tends to stay in the vicinity of the original chloride ion. In the ONIOM calculations, $Cl^- + CH_3Cl$ was considered as the ''model'' system and was handled with the ''high-level'' method, while the explicit water molecule in the microsolvated complex was treated at the ''low-level''. The molecular orbital (MO) and ONIOM(MO:MO) calculations allow us to assess the errors introduced by the ONIOM extrapolation, as well as the effects of microsolvation on the potential-energy surfaces. We find that ONIOM[B3LYP/6-31 + G(d,p):HF/6-31 + G(d,p)] and ONIOM[B3LYP/6-31 + G(d,p):HF/6-31 + G(d,p)]-PCM methods are good approximations to the target B3LYP/6-31 + G(d,p) and B3LYP/6-31 + G(d,p)-PCM methods. In addition, several approximate (computationally less expensive) schemes in the ONIOM-PCM method have been compared to the exact scheme, and all are shown to perform well.

Keywords: Hybrid method – Polarizable continuum method – Our own *N*-layered integrated molecular orbital and molecular mechanics – S_N2 reaction – Solvation – ONIOM – PCM

Contribution to the Jacopo Tomasi Honorary Issue

Correspondence to: Keiji Morokuma
e-mail: morokuma@emory.edu

Introduction

In recent years there has been much attention for the theoretical study of properties and reactivity of solvated systems. For this purpose a wide variety of methods have been developed and these can be divided into two main classes: the ''discrete'' or ''cluster'' approach, which maintains the molecular nature of the solvent, and the ''continuum'' approach, in which a macroscopic description of the solvent is used [1]. The discrete approach is commonplace in molecular dynamics or Monte Carlo simulations, where the solute is embedded in a box filled with explicit solvent molecules. When just a small number of solvent molecules are included, for example, in high-level quantum mechanical (QM) calculations, the approach is usually referred to as microsolvation. In the continuum approach, the solvent is represented by a reaction field that interacts with the solvent. The form of this reaction field, and its interaction with the solute, has become increasingly sophisticated over the last decades.

The discrete and continuum approaches can be applied simultaneously. It appears that a QM-continuum description of a solvated system can often be improved by including a small number of explicit solvent molecules in the QM cluster, especially when hydrogen bonds or other strong interactions exist between the solute and solvent. Correctly applying such a mixed approach ensures that the short-range and medium-range solvent–solute interactions are accurately described by the microsolvated cluster, while the long-range interactions are appropriately included via the continuum.

Particularly suitable for microsolvation studies is our own *N*-layered integrated molecular orbital and

molecular mechanics (ONIOM) hybrid method, which is a general scheme that allows one to combine different computational levels into one calculation [2, 3, 4, 5, 6, 7]. Usually, a high-level QM method is employed for the part of the system where the reaction or process takes place (the solute in this case), while a low-level QM method is used for the remainder of the system (here the solvent). Furthermore, we have extended the ONIOM method to incorporate solvent effects via the integral equation formalism (IEF) version [8] of the polarizable continuum model (PCM) method [9], which we call ONIOM-PCM [7]. With this method we can treat the process that takes place in the solute at an appropriately high computational level, microsolvate the solute at a lower level to describe the short-range solvent effects, and incorporate the long-range solvent effects via the continuum. We believe that with this scheme we can model solvated systems much more accurately, or with much greater computational efficiency, than by the PCM and/or microsolvation alone. Although a study has been published on its use [10], in the current paper we present the first systematic study of the combination of the microsolvation and continuum approach using the ONIOM-PCM method and its various approximations.

The process to which we apply the ONIOM-PCM method is the nucleophilic substitution reaction [11] of methyl chloride with a chloride anion in water.

$$(Cl^- + CH_3Cl')(H_2O) \rightarrow (CH_3Cl + Cl'^-)(H_2O).$$

This reaction has been studied extensively in both the gas phase and solvated phase using a variety of theoretical methods [12, 13, 14, 15, 16, 17]. The ion-dipole complex is stable in the gas phase, which results in a double-well energy profile for this reaction. In most polar solvents, however, the complex is not or is only just stable.

In the next sections we first summarize the ONIOM, PCM, and ONIOM-PCM methodology. We have investigated the methyl chloride S_N2 reaction with QM, ONIOM, and continuum methods, with and without microsolvation with one water molecule. In our previous work, we developed four different ONIOM-PCM schemes, with various degrees of approximation, and we specifically look into the performance of these schemes.

Methods

Our own N-layered integrated molecular orbital and molecular mechanics hybrid method (ONIOM)

The ONIOM hybrid method can partition a system into two or more layers, which can then each be treated at a different computational level. The formulation of ONIOM as an extrapolation scheme allows the combination of molecular orbital (MO) with molecular mechanics (MM) methods, as well as MO with MO methods. Most other hybrid methods are formulated as a summation scheme, and can combine only MO methods with MM methods. In the current work we combine two MO methods, for which the ONIOM energy expression can be written as

$$E^{\mathrm{ONIOM2}} = E^{\mathrm{model,high}} + E^{\mathrm{real,low}} - E^{\mathrm{model,low}}. \quad (1)$$

Real refers to the full system, which needs to be calculated only at the low computational level, while the model needs to be calculated at both the high and the low computational level. In our solute–solvent system there is no bonded interaction between the high-level layer (the solute) and the low-level layer (the solvent), and the model system is the same as the high-level layer. When bonded interaction exists between the layers, the resulting dangling bonds in the model system are saturated with link atoms.

The gradient can also be written as an extrapolation:

$$\frac{\partial E^{\mathrm{ONIOM2}}}{\partial \lambda} = \frac{\partial E^{\mathrm{model,high}}}{\partial \lambda} + \frac{\partial E^{\mathrm{real,low}}}{\partial \lambda} - \frac{\partial E^{\mathrm{model,low}}}{\partial \lambda}. \quad (2)$$

The second derivatives can be expressed in a similar fashion. Because the ONIOM potential-energy surface is well defined, and has the correct number of degrees of freedom, any conventional theoretical method for the investigation of potential-energy surfaces can be used with ONIOM. Besides the potential-energy surface, also properties and densities can be obtained in the ONIOM scheme. The integrated charge density, ρ^{ONIOM}, is used in the ONIOM-PCM methods discussed later:

$$\rho^{\mathrm{ONIOM2}} = \rho^{\mathrm{model,high}} + \rho^{\mathrm{real,low}} - \rho^{\mathrm{model,low}}. \quad (3)$$

Integral equation formalism polarizable continuum model

In the IEF-PCM method, the solvent is represented by a homogeneous polarizable continuum medium with permittivity, and the solute is represented in terms of a charge density contained by a cavity built in the medium. For such a system the basic electrostatic relation to be considered is

$$-\mathrm{div}[\varepsilon(x)\nabla V(x)] = 4\pi\rho(x), \quad (4)$$

With the macroscopic dielectric constant of the solvent $\epsilon(x) = \epsilon$ outside the cavity and $\epsilon(x) = 1$ inside the cavity. We exploit an IEF to solve Eq. (4) and to evaluate the related electrostatic potential. In this framework, the solution of the equation is given by the sum of two electrostatic potentials, one produced by a three-dimensional charge distribution, $\rho(y)$, and the other due to a charge distribution, $\sigma(y)$, placed on the cavity surface, S. The latter charge distribution arises from the polarization of the dielectric medium.

$$V(x) = V_r(x) + V_s(x) = \int_{R^3} \frac{\rho(y)}{|x-y|}\mathrm{d}y + \int_S \frac{\sigma(y)}{|x-s|}\mathrm{d}s \quad (5)$$

The integral in the first term is taken over the entire three-dimensional space, whereas the second integration is over the cavity surface.

The problem is thus shifted to the evaluation of the apparent surface charge (ASC) density, $\sigma(y)$. We now partition the surface into small portions (called tesserae) of known area, and assume that the apparent charge density is constant on each of them. In this framework, which is very similar to the boundary element method used in physics and engineering, the integral form of $V_s(x)$ in Eq. (5) is reduced to a finite sum running over the point charges representing the surface charge. The relations determining the apparent charges, $\mathbf{q}$, can be expressed in the form of a matrix equation:

$$\mathbf{q} = -\mathbf{Q}\mathbf{V}_\mathbf{n}, \quad (6)$$

where $\mathbf{V}_n$ is a column matrix containing the solute electrostatic potentials on the tesserae, and $\mathbf{Q}$ is a square matrix with dimension

equal to the number of tesserae and with elements depending on geometrical cavity parameters and the solvent dielectric constant ϵ.

The generalization of IEF to QM calculations is achieved by defining an effective Hamiltonian, i.e., a Hamiltonian to which solute–solvent interactions are added in terms of a solvent reaction potential, namely,

$$H^{\text{eff}}|\Phi_0> = (H_0 + V_{\text{int}})|\Phi_0>, \tag{7}$$

where H_0 is the Hamiltonian of the isolated molecule and V_{int} describes the response function of the reaction potential associated with the solvent. The solute–solvent interaction is represented by terms that can be generalized as products:

$$V_{\text{int}} \rightarrow \mathbf{V}^{\dagger}\mathbf{q}.$$

$\mathbf{V}^{\dagger}$ indicates the transpose of the matrix containing the solute potential on the tesserae.

The introduction of the solvent terms in the Hamiltonian requires the definition of the functional to be minimized in a standard variational scheme. Here this is the free-energy functional G_{es}, where the index es indicates that we only consider the electrostatic interactions between solute and solvent:

$$G_{\text{es}} = \langle\Psi|H_0|\Psi\rangle + \frac{1}{2}\langle\Psi|V_{\text{int}}|\Psi\rangle. \tag{8}$$

Own N-layered integrated molecular orbital and molecular mechanics polarizable continuum model

As already shown, for the electrostatic part of the IEF-PCM method the wave function and the ASC are mutually equilibrated. Conceptually this can be quite easily incorporated in the ONIOM scheme. We define the cavity based on the real system, and carry out each of the three ONIOM subcalculations in the reaction field resulting from the cavity surface charge distribution. This charge distribution depends on the electrostatic potential at the cavity surface from the QM charge density, which can be obtained in the ONIOM scheme according to Eq. (3). In other words, ONIOM can provide the QM charge density that IEF-PCM requires to evaluate the reaction field, which in turn is suitable without modifications for the ONIOM calculation. However, in standard IEF-PCM calculations, the wave function and ASC are optimized simultaneously [18]. This is no longer possible with the ONIOM-PCM scheme as outlined earlier. Only after the three subcalculations are completed, the integrated charge density can be obtained and used in the IEF-PCM part of the scheme. This results in a double-iteration scheme, which in fact was used in the original PCM implementations. Since generally such an optimization is computationally less efficient than a simultaneous optimization scheme, we investigated approximations to the ONIOM-PCM scheme that avoid the use of a double-iteration optimization of the wave function and ASC. This led to the four different ONIOM-PCM schemes documented in Ref. [7], which we will briefly summarize here, and are schematically represented in Fig. 1.

ONIOM-PCM/A,

$$E^{\text{ONIOM-PCM/A}} = E^{\text{model,high}}\left(\rho^{\text{integrated}}\right) + E^{\text{real,low}}\left(\rho^{\text{integrated}}\right) - E^{\text{model,low}}\left(\rho^{\text{integrated}}\right)$$

This is the "exact" ONIOM-PCM scheme as outlined earlier, and requires the computationally expensive double-iteration scheme. The cavity is based on the real system, and is used in each of the three ONIOM subcalculations. Only one set of ASCs, $\rho^{\text{integrated}}$, is used, which is determined and used by each of the subcalculations. This coupling between the subcalculations is represented by the double arrows in Fig. 1, and is the reason for the requirement of the double-iteration ASC/wave function optimization, and are schematically represented in Fig. 1

ONIOM-PCM/B.

$$E^{\text{ONIOM-PCM/B}} = E^{\text{model,high}}\left(\rho^{\text{real,low}}\right) + E^{\text{real,low}}\left(\rho^{\text{real,low}}\right) - E^{\text{model,low}}\left(\rho^{\text{real,low}}\right)$$

We assume that the reaction field determined at the low level for the real system is a good approximation for the integrated reaction field in ONIOM-PCM/A. The ASC is determined by $\rho^{\text{low,real}}$, the density at the low level on the real system, via a regular efficient IEF-PCM calculation, and is subsequently used in the two model system calculations, and are schematically represented in Fig. 1

ONIOM-PCM/C.

$$E^{\text{ONIOM-PCM/C}} = E^{\text{model,high}} + E^{\text{real,low}}\left(\rho^{\text{real,low}}\right) - E^{\text{model,low}}$$

The solvent effect is included only at the low computational level for the real system. The model system calculations are carried out for a vacuum. The assumption is that the extrapolation to the high level is not affected by the reaction field, and are schematically represented in Fig. 1

ONIOM-PCM/X.

$$E^{\text{ONIOM-PCM/X}} = E^{\text{model,high}}\left(\rho^{\text{model,high}}\right) + E^{\text{real,low}}\left(\rho^{\text{real,low}}\right) - E^{\text{model,low}}\left(\rho^{\text{model,low}}\right)$$

This method does not fit in the hierarchy of ONIOM-PCM/A, B, and C. We still use one cavity, based on the real system, but each of the subcalculations has its own ASC. In a sense it can be regarded as an alternative to the exact ONIOM-PCM/A, but not as a simplification.

Computational detailsWe have implemented the ONIOM-PCM evaluation of the energy and its first geometrical derivatives in a private development version of the Gaussian 99 program [19]. Unless noted, the reported energies were obtained using geometries optimized at the respective level of theory. However, the gradient calculation in the IEF-PCM (and ONIOM-PCM) code that was used is not fully consistent with the energy surface. This is usually not a problem, but did show up in the geometry optimization of monohydrated transition state with a continuum. The reason is that the interaction between the water molecule and the solute is very weak in this complex, which makes the optimization very sensitive to numerical instabilities. We used the convergence criteria based on the calculated gradients. In the ONIOM and ONIOM-PCM calculations we used B3LYP with the 6-31 + G(d,p) basis set as the high level and Hartree–Fock (HF) with the same basis set as the low level. Since analytical second derivatives were not available for ONIOM-PCM, only the gas-phase critical points were checked for the correct curvature of the potential surface and the zero-point energy correction (ZPC) was calculated.

IEF-PCM was used for the continuum calculations, without inclusion of the nonelectrostatic contributions. The latter is acceptable because the primary goal of the current work is to compare the ONIOM-PCM approximations to the target MO-PCM results, and not to experimental data. The cavities used in IEF-PCM were defined as interlocking spheres centered on the nuclei, with van der Waals radii scaled by a factor of 1.2. The solvent represented by the continuum is water, for which a standard dielectric constant, e, of 78.39 was used.

Results and discussion

Gas phase

Before interpreting the ONIOM-PCM results, we briefly discuss the reaction without the PCM, mainly as the calibration point for calculations with the PCM. For the

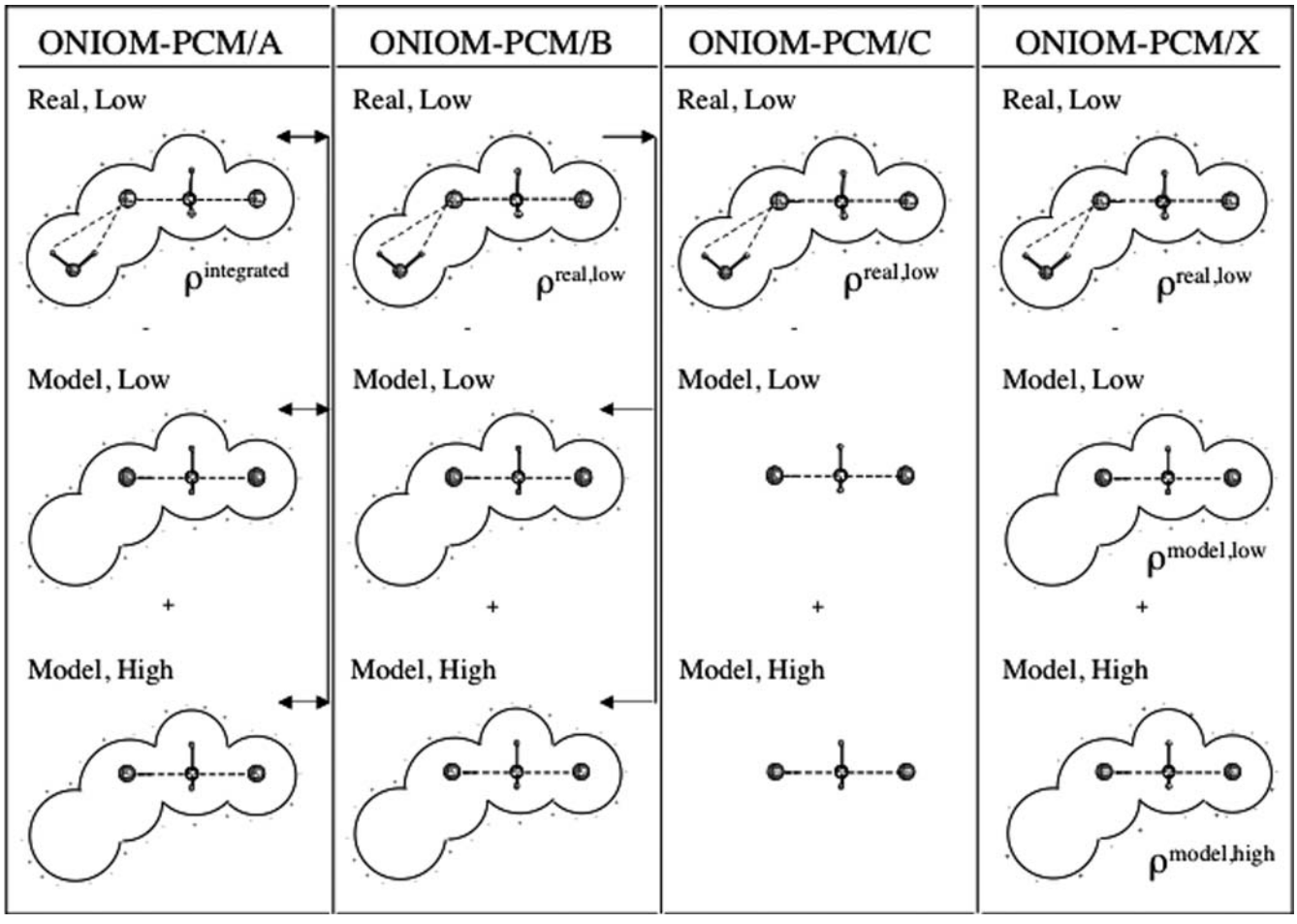

Fig. 1. Schematic representation of the four different own *N*-layered integrated molecular orbital and molecular mechanics (*ONIOM*) polarizable continuum model (*PCM*) schemes

reaction without water, we denote the chloride ion, methyl chloride, and transition state as Cl, MeCl, and TS, respectively, while the ion–methyl chloride complex is denoted as Cl–MeCl. For the reaction with the water molecule, the hydrated ion, the complex, and the transition state are denoted as WCl, WCl–MeCl and WTS, respectively. In the ONIOM calculations, the water molecule is the low-level layer. The structures of these species are shown in Fig. 2, with selected geometrical parameters in Table 1. The HF and B3LYP results agree with previous studies reported at these levels [15, 16, 17]. At the ONIOM level, parameters that involve high-level atoms are similar to the B3LYP values, while parameters that involve only low-level atoms are similar to the corresponding HF values. This is as expected from the definition of the method. One also notes that the imaginary frequency of the hydrated transition state at the ONIOM level is similar to that at the B3LYP level.

The relative energies in the gas phase are shown in Table 2. For the system without water, B3LYP accurately reproduces both the experimental complexation energy E_C (−9.6 kcal/mol computed with ZPC versus −8.6 or −12.2 kcal/mol experimental [20, 21]) and the near-zero barrier [22, 23] E_{TS} (−1.5 kcal/mol computed with ZPC). At the HF level, the complexation energy (–8.8 kcal/mol with ZPC) agrees with experiment, but the barrier (6.1 kcal/mol with ZPC) is overestimated. Upon hydration, for all the methods, the complexation energy $E_C(W)$ is reduced and the barrier $E_{TS}(W)$ is raised, which is what we expect on the basis of the experimental value for the barrier in water (26.5 kcal/mol) [24] and the disappearance of the ion-dipole complex. The ONIOM barrier is about 1 kcal/mol lower than the B3LYP barrier, which is an error slightly larger than what ONIOM is usually capable of. This is due to hydrogen bonding being included at the HF (low) level, which is not able to reproduce B3LYP very well. In fact, hydrogen bonding is often a difficult issue in ONIOM studies, and has been the topic of several previous studies [25, 26]. We also see in Table 1 that the hydrogen-bonding distances are about 10% larger at the HF (and ONIOM) level than at the B3LYP level. Finally, in Table 2 we show the hydration energies, E_W. Because these are determined mainly at the low level, ONIOM and HF yield nearly identical results. They do not, however, reproduce the B3LYP values, or even the trend in the B3LYP values. The latter is the root of the 1-kcal/mol error in the ONIOM barrier relative to B3LYP.

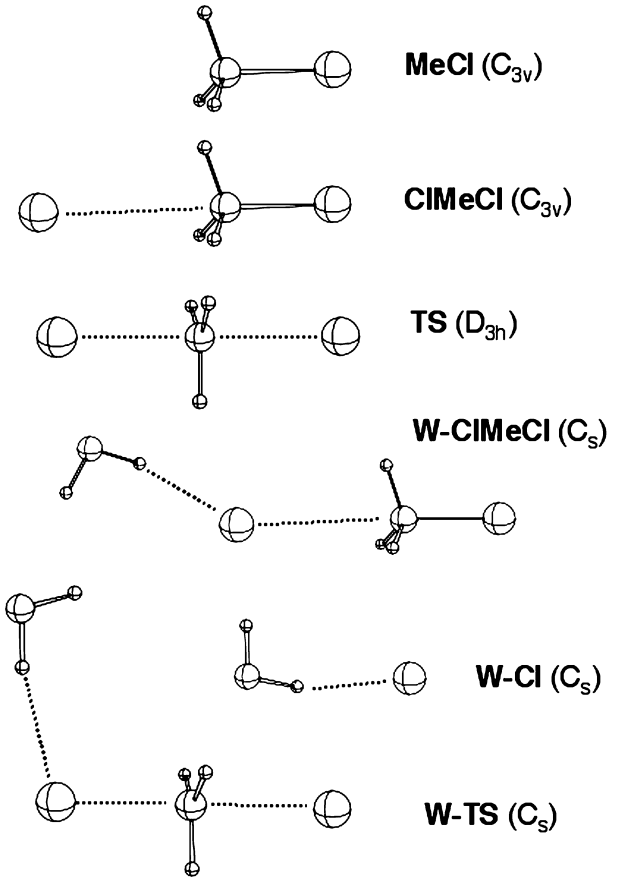

Fig. 2. Gas-phase structures and their symmetries of the reactants, intermediates and transition states, with and without one explicit water molecule

Table 1. Selected geometrical parameters (distances in angstroms, angles in degrees, and transition state frequency in imaginary reciprocal centimeters) of the structures optimized for the gas phase at different theoretical levels. See Fig. 2 for definitions of the parameters

Structures	Parameters	HF	B3LYP	ONIOM
MeCl	Cl–C	1.79	1.81	
Cl–MeCl	Cl–C	3.36	3.19	
	Cl′–C	1.82	1.86	
TS	Cl–C	2.40	2.37	
	Frequency	425i	347i	
WCl	Cl–H	2.40	2.190	2.40
	Cl–H–O	156.4	164.2	156.4
WCl–MeCl	Cl–C	3.37	3.240	3.21
	Cl′–C	1.82	1.85	1.85
	Cl–H	2.42	2.21	2.42
	C–Cl–H	165.9	145.8	164.2
	Cl–H–O	156.1	164.3	156.1
WTS	C–C	2.34	2.30	2.29
	Cl′–C	2.45	2.44	2.45
	Cl–H	2.54	2.31	2.54
	C–Cl–H	129. 6	105.7	122.2
	Cl–H–O	157.9	168.3	159.1
	Frequency	419	340	338

Solution phase with fixed geometries

We first calculated the solution-phase barrier at the various levels with PCM (HF-PCM, B3LYP-PCM, ONIOM-PCM/A, B, C and X) using the gas-phase B3LYP optimized geometries discussed in the previous section. Although the neglect of the geometrical relaxation may lead to significant "chemical errors", it is useful to illustrate the performance of the four ONIOM-PCM schemes.

The barriers in solution for the nonhydrated solute, E_{TS}, and for the monohydrated solute, $E_{TS}(W)$, are shown in Table 3. Since the ion-dipole complex does not exist in solution, we did not calculate its complexation energy. We also computed ONIOM-PCM values for the reaction without explicit water molecules. In this case, there is no low-level layer (the water molecule) and the "model" system is the same as the "real" system. In ONIOM-PCM/A, $\rho^{\text{integrated}}$ is then the same as ρ^{B3LYP}, and $E^{\text{real,low}}(\rho^{\text{B3LYP}})$ and $E^{\text{model,low}}(\rho^{\text{B3LYP}})$ cancel out so the final result is $E^{\text{model,high}}(\rho^{\text{B3LYP}}) = E^{\text{B3LYP}}(\rho^{\text{B3LYP}})$, which is identical to the B3LYP-PCM result. ONIOM-PCM/X also becomes the same as B3LYP-PCM. On the other hand, in ONIOM-PCM/B and C the reaction field is calculated only at the low level (HF) of theory, giving $E^{\text{B3LYP}}(\rho^{\text{HF}})$ and $E^{\text{HF}}(\rho^{\text{HF}}) + E^{\text{B3LYP}} - E^{\text{HF}}$, respectively. The HF-PCM method gives $E^{\text{HF}}(\rho^{\text{HF}})$.

Most striking aspect is that the HF barriers of 27.4 and 24.8 kcal/mol are in quite good agreement with the experimental value in water of 26.5 kcal/mol, while B3LYP underestimates the barrier by at least 6 kcal/mol. Similar calculations by Mohamed and Jensen [15], but with inclusion of nonelectrostatic contributions, yielded the same discrepancy with experiment. In addition, they found that inclusion of more explicit water molecules does not significantly modify the barrier. On the basis of these results, and the fact that B3LYP reproduces the experimental gas phase results well, the error is most likely due to either to the B3LYP-PCM description of the solvent or to the neglect of geometrical relaxation.

From Table 3 we see that the ONIOM-PCM results for the monohydrated system are 1–2 kcal/mol lower than the "target" B3LYP-PCM value. However, in order to assess the performance of the ONIOM-PCM schemes, we must take into account that there are a number of contributions to this error. First, in Table 2 we saw that gas-phase ONIOM(B3LYP:HF) introduces an error of 1.1 kcal/mol relative to gas-phase B3LYP, and it is clear that this error will propagate into the ONIOM-PCM results. Second, in ONIOM-PCM, the solvent PCM effect is partially included at the B3LYP level, and partially at the HF level, and whether the B3LYP solvent effect is reproduced accurately depends on the partitioning and method combination. Third, only ONIOM-PCM/A is fully consistent with respect to both the ONIOM the scheme and the PCM scheme; ONIOM-PCM/B, C, and X are approximations to ONIOM-PCM/A.

Table 2. Gas-phase complexation energies of the ion-dipole complex, E_C, and transition state, E_{TS} (relative to the reactants) with (*W*) and without one explicit water molecule, and the micro solvation energies of the chloride, E_W (Cl), the ion-dipole complex, E_W(Cl–MeCl), and transition state, E_W (TS), at different theoretical levels. All energies are in kilocalories per mole

Energies	Definition	Without zero-point correction			With zero-point correction		
		HF	B3LYP	ONIOM	HF	B3LYP	ONIOM
E_C	E(Cl–MeCl)−[E(Cl) + E(MeCl)]	−8.96	−9.64		−8.76	−9.55	
E_{TS}	E(TS)−[E(Cl) + E(MeCl)]	6.43	−1.05		6.06	−1.47	
E_C(W)	E(WCl–MeCl)−[E(WCl) + E(MeCl)]	−8.28	−8.45	−8.89	−8.07	−8.18	−8.77
E_{TS}(W)	E(WTS)−[E(WCl) + E(MeCl)]	10.64	4.39	3.31	10.17	4.16	2.79
E_W(Cl)	E(WCl)−[E(W) + E(Cl)]	−12.38	−14.80	−12.38	−11.01	−13.62	−11.01
E_W(Cl–MeCl)	E(WCl–MeCl)−[E(W) + E(Cl–MeCl)]	−11.70	−13.61	−11.63	−10.31	−12.25	−10.23
E_W(TS)	E(WTS)−[E(W) + E(TS)]	−8.17	−9.36	−8.02	−6.89	−7.98	−6.75

Table 3. Fixed geometry barriers, E_{TS}, (kcal/mol, relative to the reactants) in the aqueous solution with and without one explicit water molecule, calculated with various polarizable continuum model methods.Gas-phase B3LYP-optimized geometries are used

Method	E_{TS}	E_{TS}(W)	Solvation
HF-PCM	27.36	24.75	14.24
B3LYP-PCM	20.60	19.49	15.11
ONIOM-PCM/A	20.60	18.29	15.12
ONIOM-PCM/B	20.89	18.53	15.36
ONIOM-PCM/C	19.88	17.42	14.24
ONIOM-PCM/X	20.60	17.97	14.80

In the last column of Table 3 we show the solvation effect on the barrier for the monohydrated system, which is defined as the difference between the solution-phase barrier (in Table 3) and the gas-phase barrier, both at the B3LYP gas-phase geometries. This quantity no longer includes the "gas-phase ONIOM(B3LYP:HF)" contribution to the total error as described in the previous paragraph. We see that the B3LYP and ONIOM values only differ by 0.01 kcal/mol, which shows that ONIOM-PCM is very well able to reproduce the B3LYP solvation effect for the current reaction. Of the approximations to ONIOM-PCM/A, scheme B overestimates, and scheme C underestimates the solvation effect in both the nonhydrated and the monohydrated case, which is as expected and is the same trend as observed in the previously published ONIOM-PCM study. ONIOM-PCM/X approaches ONIOM-PCM/A quite well.

Solution phase with geometrical relaxation

We carried out geometry optimization of the reactants (WCl + MeCl) and transition states (WTS) with one explicit water molecule in the solution phase using the ONIOM-PCM/A, B, C and X methods as well as the HF-PCM and B3LYP-PCM methods. We also optimized the structure of the nonhydrated structures without explicit solvent molecules in solution. The results of optimized geometries in solution are reported in Fig. 3 and Table 4. Again, the ONIOM parameters in

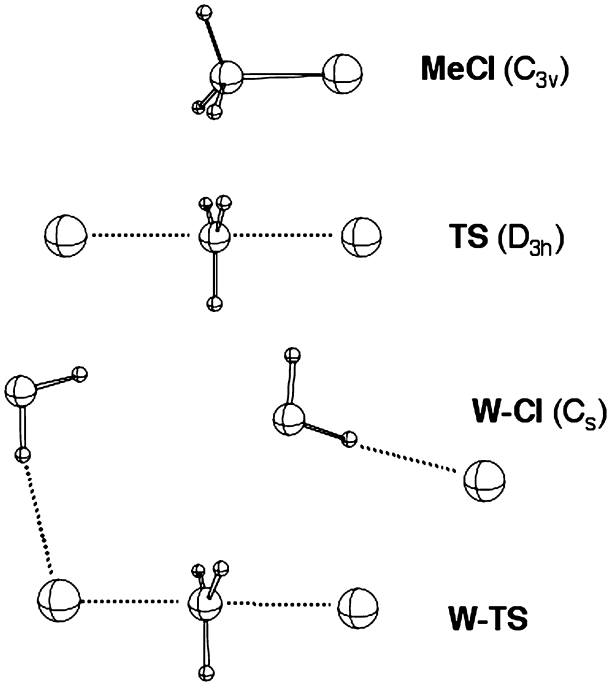

Fig. 3. Solution-phase structures and their symmetries of the reactants, intermediates and transition states, with and without one explicit water molecule

the low-level region follow the HF values, and the parameters in the high-level region (Cl–C and Cl′–C) are close to the B3LYP values. There are, however, larger differences between the ONIOM-PCM values and their HF or B3LYP counterparts than we see in the gas-phase results in Table 1, and these are due to the additional level of coupling between the two layers via the reaction field. Because this coupling is included in a different way in each of the ONIOM-PCM schemes, there is a small variation of the geometrical parameters between the different ONIOM-PCM schemes. However, the differences of different ONIOM-PCM approximation schemes (B, C and X) from the exact ONIOM-PCM/X scheme are still rather small in the present system, and we have to conclude that all the ONIOM-PCM approximate schemes are working well.

Table 4. Selected geometrical parameters (distances in angstroms and angles in degrees) of the structures optimized for aqueous solution at different theoretical levels. See Fig. 3 for definitions of the parameters

		HF-PCM	B3LYP-PCM	ONIOM-PCM/A	ONIOM-PCM/B	ONIOM-PCM/C	ONIOM-PCM/X
MeCl	Cl–C	1.80	1.82	1.82	1.82	1.82	1.82
TS	Cl–C	2.41	2.36	2.36	2.37	2.38	2.36
WCl	Cl–H	2.36	2.17	2.34	2.35	2.36	2.35
	Cl–H–O	177.0	178.3	176.8	177.0	178.0	177.1
WTS	Cl–C	2.39	2.33	2.34	2.34	2.36	2.34
	Cl′–C	2.42	2.39	2.38	2.39	2.40	2.38
	Cl–H	2.47	2.28	2.46	2.46	2.47	2.46
	C–Cl–H	88.4	86.0	89.3	92.0	88.3	90.3
	Cl–H–O	174.4	176.9	176.1	175.1	174.2	174.7
	H–C–Cl–H	−171.8	−170.6	−175.1	−171.6	−172.2	−170.7
	Cl–H–O–H	38.2	55.4	42.3	31.0	38.0	35.0

Table 5. Barriers, E_{TS}, (kcal/mol, relative to the reactants) in aqueous solution and their differences, ΔE_{TS}, from the gas-phase values in Table 2 (or the solvation effect) as well as the relaxation and interaction contributions to ΔE_{TS}, with and without one explicit water molecule, calculated with the various ONIOM-PCM methods

	Method	E_{TS} or E_{TS}(W)	ΔE_{TS} or ΔE_{TS}(W)	Deformation	Interaction
No H_2O	HF-PCM	27.22	20.78	–0.01	20.79
	B3LYP-PCM	20.61	21.65	0.00	21.65
	ONIOM-PCM/A	20.61	21.65	0.00	21.65
	ONIOM-PCM/B	20.89	21.93	0.00	21.94
	ONIOM-PCM/C	19.85	20.90	–0.01	20.91
	ONIOM-PCM/X	20.61	21.65	0.00	21.65
With H_2O (W)	HF-PCM	26.39	15.75	0.17	15.58
	B3LYP-PCM	20.26	15.87	0.16	15.70
	ONIOM-PCM/A	19.91	16.60	0.08	16.52
	ONIOM-PCM/B	20.09	16.78	–0.02	16.80
	ONIOM-PCM/C	19.05	15.74	0.05	15.69
	ONIOM-PCM/X	19.62	16.31	0.04	16.28

The activation energies, E_{TS} and E_{TS}(W), with geometry relaxation are shown in Table 5, i.e., at respectively optimized geometries in solution for each scheme. We also show the solvation effect on the barrier, ΔE_{TS} and ΔE_{TS}(W), i.e., the differences in the activation energies between the solution in Table 3 and the gas phase in Table 2, all at respectively optimized geometries. In the previous section we separated the solvation aspect (fixed at gas-phase optimized geometries) and the "ONIOM aspect", in order to assess the performance of ONIOM-PCM. Now we have optimized the structures in solution, we can separate the solvation effect into the deformation contribution and the interaction contribution. The deformation contribution is the gas-phase energy for the structure optimized for solution, E(gas//solution), minus the gas-phase energy for the optimized structure in the gas phase, E(gas//gas), and represents how the change in geometry upon solvation changes the reaction barrier, ΔE_{TS} and ΔE_{TS}(W), in the gas phase. While the deformation contribution is negligible for the nonhydrated (without explicit water) reaction, that for the hydrated (with explicit water) reaction is small but nonzero. This suggests that it originates from the geometrical changes of the water molecule between the transition state and the reactant. We see that again the ONIOM-PCM/B and ONIOM-PCM/C schemes overestimate and under estimate, respectively, the solvation aspect of ONIOM-PCM/A, and that ONIOM-PCM/X is reasonably close.

Conclusions

From the current study it is clear that the ONIOM-PCM scheme has the potential to make solution-phase calculations feasible for very large systems. For a given geometry, ONIOM-PCM/A reproduced the solvation effect of the target B3LYP-PCM calculation nearly exactly. There is still an error with respect to the target calculation that does not involve the "solvation aspect", but it is due to the poor description of hydrogen bonding of the current ONIOM partitioning and method combination. Besides the direct contribution to the error, the poor hydrogen-bonding description also results in a geometrical error, which indirectly contributes to the error because the solvation calculation is very sensitive to it. Improvement of the accuracy must therefore be sought in a better ONIOM partitioning and method combination, and not in the coupling of the ONIOM and PCM schemes.

The ONIOM-PCM approximations B and C perform reasonable well, overestimating and underestimating ONIOM-PCM/A in the same way as observed in the previous ONIOM-PCM study. ONIOM-PCM/X also performs well, but may not be systematic enough to be used as a reliable alternative to ONIOM-PCM/A. The current results encourage us to investigate efficient algorithms for ONIOM-PCM/A that avoid or increase the efficiency of the double-iteration scheme for the optimization of the wave function and ASC. In

addition, the development of efficient algorithms for MM with the PCM will make it possible to carry out large QM/MM calculations for the solvated phase [27].

Acknowledgements. The present research is in part supported by a grant (CHE-0209660) from the National Science Foundation and a grant from Gaussian, Inc. Acknowledgement is also made to the Cherry L. Emerson Center of Emory University for the use of its resources, which is in part supported by a National Science Foundation grant (CHE-0079627) and an IBM Shared University Research Award.

References

1. (a) Tomasi J, Persico M (1994) Chem Rev 94:2027; (b) Cramer CJ, Truhlar DG (1999) Chem Rev 99:2161
2. Maseras F, Morokuma K (1995) J Comput Chem 16:1170
3. Svensson M, Humbel S, Froese RDJ, Matsubara T, Sieber S, Morokuma K (1996) J Phys Chem 100:19357
4. Humbel S, Sieber S, Morokuma K (1996) J Chem Phys 16:1959
5. Dapprich S, Komáromi K, Byun KS, Morokuma K, Frisch MJ (1999) J Mol Struct (THEOCHEM) 461–462:1
6. Vreven T, Morokuma K (2000) J Comput Chem 16:1419
7. Vreven T, Mennucci B, da Silva CO, Morokuma K, Tomasi J (2001) J Chem Phys 115:62
8. (a) Cancès E, Mennucci B, Tomasi J (1997) J Chem Phys 107:3032; (b) Mennucci B, Cancès E, Tomasi J (1997) J Phys Chem B 101:10506; (c) Cancès E, Mennucci B (1998) J Math Chem 23:309
9. (a) Miertus S, Scrocco E, Tomasi J (1981) Chem Phys 55:117; (b) Cammi R, Tomasi J (1995) J Comput Chem 16:1449
10. Mennucci B, Martínez, JM, Tomasi J (2001) J Phys Chem A 105:7287
11. Shaik S, Schlegel HB, Wolfe S (1992) Theoretical aspects of physical organic chemistry. The S_N2 mechanism. Wiley, New York
12. Cossi M, Adamo C, Barone V (1998) Chem Phys Lett 297:1
13. Morokuma K (1982) J Am Chem Soc 104:3732
14. Truong T, Stefanovich E (1995) J Phys Chem 99:14700
15. Mohamed AA, Jensen F (2001) J Phys Chem A 103:3259
16. Okuno Y (1996) J Chem Phys 105:5817
17. Asada T, Kato K, Kitaura K (1999) J Mol Struct (THEOCHEM) 461–462:493
18. Cossi M, Barone V, Cammi R, Tomasi J (1996) Chem Phys Lett (1996) 255:327
19. Frisch MJ, Trucks GW, Schlegel HB, Scuseria GE, Robb MA, Cheeseman JR, Zakrzewski VG, Montgomery JA Jr, Stratmann RE, Burant JC, Dapprich S, Millam JM, Daniels AD, Kudin KN, Strain MC, Farkas O, Tomasi J, Barone V, Cossi M, Cammi R, Mennucci B, Pomelli C, Adamo C, Clifford S, Ochterski J, Petersson GA, Ayala PY, Cui Q, Morokuma K, Malick DK, Rabuck AD, Raghavachari K, Foresman JB, Cioslowski J, Ortiz JV, Stefanov BB, Liu G, Liashenko A, Piskorz P, Komaromi I, Gomperts R, Martin RL, Fox DJ, Keith T, Al-Laham MA, Peng CY, Nanayakkara A, Gonzalez C, Challacombe M, Gill PMW, Johnson B, Chen W, Wong MW, Andres JL, Head-Gordon M, Replogle ES, Pople JA (1998) Gaussian 98 (revision A.1). Gaussian, Pittsburgh, PA
20. Larson JW, McMahon TB (1984) J Am Chem Soc 106:517
21. Dougherty RC, Dalton J, Roberts JD (1974) Org Mass Spectrom 8:77
22. Han C-C, Dodd JA, Brauman JI (1986) J Phys Chem 90:471
23. Gonert S, DePuy CH, Bierbaum VM (1991) J Am Chem Soc 113:4009
24. Albery WJ, Kreevoy, MM (1978) Adv Phys Org Chem 16:87
25. Re S, Morokuma K (2001) J Phys Chem A 105:7185
26. Tschumper GS, Morokuma K (2002) J Mol Struct (THEOCHEM) 592:137
27. Cui Q (2002) J Chem Phys 117:4720